12-2023

# Environmental exposures and aging.

Daniel Chris Gomes
*University of Louisville*

# ENVIRONMENTAL EXPOSURES AND AGING

BY

Daniel Chris Gomes
B.A., Earlham College, 2018

A Thesis
Submitted to the Faculty of the
School of Medicine of The University of Louisville
In partial fulfillment of the requirements for the Degree of

Master of Science in Pharmacology and Toxicology

Department of Pharmacology and Toxicology
University of Louisville
Louisville, Kentucky

December 2023

ENVIRONMENTAL EXPOSURES AND AGING

By

Daniel Chris Gomes
B.A., Earlham College, 2018

A Thesis approved on

September 21, 2023

By the following Thesis Committee:

Timothy E. O'Toole

Petra Haberzettl

Sanjay Srivastava

David Hein

Joseph Moore IV

ACKNOWLEDGEMENTS

I would like to thank my mentor, Dr. Timothy E. O'Toole, for his unwavering guidance, support, and encouragement. I would also like to thank all members of the O'Toole laboratory, the Envirome Institute Flow core and the Medical Dental Research Animal Exposure core for their contributions and assistance. I would like to thank my brilliant committee members Dr. Petra Haberzettl, Dr. Sanjay Srivastava, Dr. David Hein, and Dr. Joseph Moore for their feedback and support. I would also like to thank my parents Vincent Gomes and Mary Rozario for believing in me and my goals and supporting me always. I would like to acknowledge my appreciation for all of the facilities and equipment at the Christina Lee Brown Envirome Institute for providing me with everything I needed to conduct my research.

ABSTRACT

ENVIRONMENTAL EXPOSURES AND AGING

Daniel Chris Gomes

September 21, 2023

In recent years, research into air pollution has shown that exposure to certain components in air pollution, primarily $PM_{2.5}$ can accelerate biological aging and thereby lead to increased susceptibility to multiple diseases. We hypothesize that prolonged exposure to air pollutants can result in premature aging leading to extensive tissue dysfunction and susceptibility to diseases. To examine this, we exposed mice to $PM_{2.5}$ for 9, 15, and 21 days, then measured the telomere lengths, cellular senescence, and histone methylation patterns of multiple cell types. We found consistently increased telomere attrition, cellular senescence and advanced age-consistent histone methylation patterns in groups exposed to $PM_{2.5}$ across all examined cell types. Our investigation provides ample evidence that exposure to $PM_{2.5}$ can cause premature aging and has the potential to lead to diseases such as cardiovascular disorders, type II diabetes, immune system dysfunction and neurodegenerative disorders.

TABLE OF CONTENTS

PAGE

LIST OF TABLES

TABLE PAGE

LIST OF FIGURES

FIGURE PAGE

# INTRODUCTION

## AIR POLLUTION

Exposure to high levels of air pollution is an increasingly growing problem in several parts of the world contributing to morbidity and mortality Polluted air derives from both natural and man-made causes that are increasing in the past century due to the growing population, rapid urbanization and industrialization, and climate change leading to increased temperatures, aridity and increased incidence of wildfires [30]. Extensive studies into air pollution in recent years has shown that several of its components can have major adverse health effects such as increased risk for type 2 diabetes [1] and cardiovascular diseases [2] such as myocardial infarction, atherosclerosis, and strokes to name a few.

There are 6 major air pollutants as designated by the United States Environmental Protection Agency (EPA) as of 2010. These are listed as “criteria” pollutants meaning that the concentrations of these pollutants in the atmosphere are measured and used to identify the overall air quality. The list includes particulate matter (PM which consists of $PM_{2.5}$ and $PM_{10}$), carbon monoxide (CO), nitrogen oxides (NO and $NO_2$), sulfur dioxide ($SO_2$), ozone ($O_3$) and lead (Pb). Table 1 shows the acceptable concentrations, environmental risks and human health risks of these pollutants [30].

| Pollutant | Common sources | Max. acceptable concentration in the atmosphere | Environmental risks | Human health risks |
|---|---|---|---|---|
| carbon monoxide (CO) | automobile emissions, fires, industrial processes | 35 ppm (1-hour period); 9 ppm (8-hour period) | contributes to smog formation | exacerbates symptoms of heart disease, such as chest pain; may cause vision problems and reduce physical and mental capabilities in healthy people |
| nitrogen oxides (NO and NO2) | automobile emissions, electricity generation, industrial processes | 0.053 ppm (1-year period) | damage to foliage; contributes to smog formation | inflammation and irritation of breathing passages |
| sulfur dioxide (SO2) | electricity generation, fossil-fuel combustion, industrial processes, automobile emissions | 0.03 ppm (1-year period); 0.14 ppm (24-hour period) | major cause of haze; contributes to acid rain formation, which subsequently damages foliage, buildings, and monuments; reacts to form particulate matter | breathing difficulties, particularly for people with asthma and heart disease |
| ozone (O3) | nitrogen oxides (NOx) and volatile organic compounds (VOCs) from industrial and automobile emissions, gasoline vapours, chemical solvents, and electrical utilities | 0.075 ppm (8-hour period) | interferes with the ability of certain plants to respire, leading to increased susceptibility to other environmental stressors (e.g., disease, harsh weather) | reduced lung function; irritation and inflammation of breathing passages |
| particulate matter | sources of primary particles include fires, smokestacks, construction sites, and unpaved roads; sources of secondary particles include | 150 $\mu g/m^3$ (24-hour period for particles <10 µm); 35 $\mu g/m^3$ (24-hour period for particles <2.5 µm) | contributes to formation of haze as well as acid rain, which changes the pH balance of waterways and damages foliage, buildings, and monuments | irritation of breathing passages, aggravation of asthma, irregular heartbeat |

| | | | | |
|---|---|---|---|---|
| | reactions between gaseous chemicals emitted by power plants and automobiles. | | | |
| lead (Pb) | metal processing, waste incineration, fossil-fuel combustion | 0.15 µg/m3 (rolling three-month average); 1.5 µg/m3 (quarterly average) | loss of biodiversity, decreased reproduction, neurological problems in vertebrates | adverse effects upon multiple bodily systems; may contribute to learning disabilities when young children are exposed; cardiovascular effects in adults |

**TABLE 1.** Summary of the 6 major air pollutants. The 6 major air pollutants as designated by the United States Environmental Protection Agency (EPA) as of 2010 showing common sources, acceptable concentrations, environmental risks and human health risks of these pollutants.
Source: U.S. Environmental Protection Agency

## PARTICULATE MATTER ($PM_{2.5}$ & $PM_{10}$)

There are several sources of air pollution which contribute the 6 major pollutants in our atmosphere. Air borne particles from increasing wildfires, volcanic eruptions and land dust can be classified under natural phenomena while vehicle exhausts, factory emissions, oil refineries and other such industrial processes can be classified as man-made sources of air pollution [3].

Adverse health effects are most strongly associated with the particulate matter fraction of air pollution. The physiological responses to PM depend upon particle size. Large particles are about 10 micrometers in diameter ($PM_{10}$) and can get deposited in the nasal, pharyngeal, and laryngeal regions. Smaller particles from 5 - 2.5 micrometers ($PM_{2.5}$) can be deposited in the tracheas while ultrafine particles are 0.1 - 2.5 micrometers and can be deposited deep within the lungs, in the alveolar sacs and ducts due to their small size [4]. There are several reports that document the link between

exposure to $PM_{2.5}$ and cardiovascular diseases [3] and type 2 diabetes [1] and in recent years there has been some interest in seeing if air pollution can also be linked to accelerated aging. An observational study done in Taiwan showed that there is a positive correlation between air pollution with skin aging in the Taiwanese population [5]. Other studies have linked $PM_{2.5}$ exposure to increased telomere shortening in truck drivers, office workers, elderly populations, and school children whose schools are located in heavily polluted areas [6-8].

Studies in more recent years have shown a direct correlation between exposure to $PM_{2.5}$ and $PM_{10}$ and telomere shortening [6, 7]. Most of the studies so far have investigated if oxidative stress caused by $PM_{2.5}$ has an effect on telomere dynamics in vitro or have reported findings from population observational studies and have shown that oxidative stress accelerates telomere shortening which causes cellular senescence [6, 7], two of the hallmarks of aging. However, these prior studies have some limitations in the fact that they only investigated leukocytes, and no other cell types, did not address any of the other hallmarks of aging and do not address mechanism or were done with only highly susceptible populations. Thus, understanding the link between $PM_{2.5}$ exposure and aging is far from complete.

## HALLMARKS OF AGING

Aging has broadly been defined as the time-dependent functional decline that affects living organisms. The more current definition of aging is the progressive loss of physiological integrity leading to impaired function and increased vulnerability to death. Aging can be a major risk factor for cancer, diabetes, cardiovascular disorders, and neurodegenerative diseases. According to current scientific literature there has been identified nine hallmarks of aging. These consist of: genomic instability due to nuclear and mitochondrial DNA damage; telomere attrition defined as the loss in telomere

length; epigenetic alterations which include DNA methylation, histone modifications (methylation and acetylation), chromatin remodeling: loss of proteostasis (i.e. impaired protein homeostasis); deregulated nutrient sensing leading to various issues in cell signaling pathways like the IGF-1, mTOR, and AMPK pathways; mitochondrial dysfunction resulting in electron leakage and reduction of ATP generation that is a consequence of increased reactive oxygen species damage; cellular senescence characterized by cell cycle arrest; stem cell exhaustion, and altered intercellular communication [9]. For our purposes we have investigated three out of the nine hallmarks of aging in our experiments which are telomere attrition, cellular senescence and histone methylation patterns.

## TELOMERES

Telomeres are structures located at the ends of linear chromosomes consisting of repetitive nucleotide sequences (TTAGGG) and associated specialized proteins. They play an important role in the protection of the terminal regions of chromosomal DNA from progressive degradation and recombination during cell proliferation and ensure the integrity of linear chromosomes. During each cell division, there is a progressive loss of a few nucleotides at the telomeres ends. Thus, telomeres shorten with age leading over time to cell cycle arrest and senescence. Telomerase is a ribonucleoprotein complex which adds species-dependent telomere repeat sequences to the 3’ end of telomeres to lengthen them thereby increasing the time it takes for the chromosomes of a cell to reach the Hayflick limit [10] which is the number of times a cell can divide before cell division stops [11]. The composition of the human telomerase complex consists of two molecules each of human telomerase reverse transcriptase (TERT), telomerase RNA (TERC), and several associated proteins which are responsible for the ensuring of

chromosomal stability by maintaining the telomere length, and allowing cells to avert senescence [12].

Studies have shown that shorter telomeres are associated with an increased risk of diseases and poor survival [10]. It has been found that telomere length can be a biomarker for cardiovascular diseases because it can be modified by inflammation and oxidative stress [13]. Owing to their high G-rich sequences telomeres are thought to be especially sensitive to oxidative damage. If not prevented, the oxidative damage of telomere regions will lead to an accumulation of damage to DNA and increased telomere loss. Telomere attrition not only arises as a consequence of aging but also results from a number of factors which include exposure to pollutants, smoking, obesity, lack of activity, unhealthy diet, and excessive stress [14].

Although oxidative damage can cause telomere shortening through double strand breaks to DNA, most telomere loss due to oxidative stress occurs during DNA replication as a result of a single strand DNA damage. As telomeric regions have low efficiency of single-strand DNA damage repair, telomeres containing such DNA damage will shorten more following the next cellular division because the sequence beyond the damage will be lost and progressive shortening will lead to cellular senescence [15].

## TELOMERASE PROTEIN (mTERT)

Nucleotide extension is accomplished at telomere ends with telomerase complex. This complex consists of an enzyme, telomerase reverse transcriptase (TERT), an RNA guide strand (TERC) and several associated proteins (Dyskerin, NOP10, NHP2, GAR-1) which serve to stabilize the interactions of TERT and TERC with the telomere end [16]. Disruptions in the expression or function of TERT, TERC or the associated proteins can result in inefficient telomere extension. Indeed, certain clinical syndromes (e.g.

Dyskeratosis congenita) characterized by shortened telomeres, are associated with aberrantly low levels of Dyskerin or other of the associated proteins [4]. Another set of proteins, the shelterin complex, is bound to the telomere end itself.

There is an emerging awareness that the cellular regulation of TERT, and hence telomere extension, can be regulated by its phosphorylation at specific residues which impact its activity and cellular localization. The human TERT protein is phosphorylated by Akt on serine 227 and 824 the former of which promotes the nuclear import of hTERT from the cytoplasm and the latter which promotes TERT activity and thus together enables telomere extension [17]. Another TERT phosphorylation is tyrosine 707 which is a substrate for c-Src. This modification has been shown to promote nuclear egress of the hTERT and thereby decrease telomere extension [4]. Interestingly, there is evidence that the kinases (Akt and Src) promoting TERT phosphorylation can be regulated by environmental exposures [18]. Hence $PM_{2.5}$-induced TERT phosphorylation may be one of the mechanisms leading to telomere shortening.

As noted above, while cellular mechanisms regulating of human TERT protein are somewhat established, less is known about regulation of mouse TERT. Indeed, many of the residues phosphorylated in the human proteins are not conserved in the mouse protein. However, Y707 is and it remains feasible that $PM_{2.5}$ exposure induces the phosphorylation of this residue, promoting nuclear egress and inefficient telomere extension and we will explore this possibility in this study.

## CELLULAR SENESCENCE

Cellular senescence is one of the nine hallmarks of aging and is defined to be a stable exit from the cell cycle in response to damage or stress [19]. Due to progressive shortening of telomeres, cells can undergo senescence. Senescent cells are viable and

metabolically active, but they display altered genes and protein expression compared to proliferating cells [20]. Senescent cells can be recognized by increased β-galactosidase (β-Gal) activity, and the secretion of pro-inflammatory factors, the senescence associated secretory phenotype (SASP). SASP can contribute to the functional disruption of tissues in an autocrine and paracrine manner leading to the senescence of neighboring cells via immunosuppression and inflammation [21]. Secreted, pro-inflammatory factors can be pathogenic and are the driving force disrupting tissue homeostasis, resulting in the loss of tissue repair and regeneration [19]. Additional characteristics of senescent cells include DNA damage [22], mitochondrial dysfunction [23], protein quality impairment [24], inflammation [25] and reactive oxygen species generation [26]. Some studies have reported that cells that have undergone telomere attrition due to $PM_{2.5}$ exposure also showed higher amounts of cellular senescence and is further evidence of their loss of function and increased susceptibility to diseases [6].

Previous studies have shown that exposure to particulate matter can lead to cellular senescence of normal lung fibroblasts via DNA damage-mediated response [27]. Other studies have shown that PM-induced senescence of skin keratinocytes involves oxidative stress-dependent epigenetic modifications [28].

## EPIGENETIC MODIFICATIONS

Epigenetic modification is the term used to refer to heritable alterations that do not arise due to changes in DNA sequences but rather are a result of modifications, or “tags”. These modifications include DNA methylation or histone modifications that alter the accessibility of the DNA and chromatin to transcriptional proteins which results in the regulation of gene expression [28].

Post translational histone modifications include methylation, acetylation, ubiquitination, ADP ribosylation, and phosphorylation which are carried out by enzymes that promote or reverse these specific modifications [29]. Aging has been associated with altered histone methylation patterns. Changes in the abundance of H3K4me3, H3K9me3, H3K27me3, H3K9ac and H4K20me3 are some of the histone modifications that have been reported to be associated with aging s [30]. In previous studies, it has been shown that H3K4me3 is a marker that is associated with active transcription and plays an important role in identifying aging and lifespan by regulating the expression of aging-related genes. H3K4me3 levels have been shown to increase with age in mouse hematopoietic stem cells (HSCs) [31]. H3K9me3 also play an important role in the aging process. Studies done in adult Drosophila midgut showed that a decrease in H3K9me3 leads to intestinal stem cell aging [32]. H3K27me3 has generally been associated with gene silencing and a more compacted heterochromatin [33]. Previous studies have shown that there is an overall loss of H3K27me3 in aged C. elegans and prematurely aged cells in patients with Hutchinson-Guildford progeroid syndrome [34]. However, mouse brains studies have shown that overall levels of H3K27me3 increase with age [35]. Studies have shown that H3K9ac levels generally decrease with age in mouse liver [36]. Finally, H4K20me3 levels has been shown to increase in senescent rat kidney cells and livers as a result of aging [37]. Due to the numerous studies performed into identifying the levels of these three histone modifications in aging, they are interesting targets to investigate in $PM_{2.5}$ exposure across different cell types.

## HYPOTHESIS

We hypothesize that with exposure to air pollution, there will be a marked decrease in telomere length, increase in cellular senescence and changes in histone methylation patterns, similar to changes that are observed as a consequence of aging.

Thus, we propose that exposure to PM can accelerate aging. To test this idea, we intend to expose mice for variable amounts of time to concentrated ambient particles (CAPS) for 6 hours daily. At the end of our exposure period, we will collect the blood and bone marrow and use it to measure telomere lengths in PBMNCs, EPCs, ckit+ bone marrow cells, and crude bone marrow cells using RT-PCR. Additionally, we will assess β-Gal activity by flow cytometry to measure the levels of cellular senescence in the same cell types. Finally, we shall also isolate histone fractions from these cells to measure the levels of histone methylation.

# MATERIALS AND METHODS

## MOUSE EXPOSURE

All mice for exposures were obtained from Jackson Laboratories and allowed to acclimate for one week after arrival at our animal facility. These mice were C57BL/6J, males at 12 weeks of age. For exposures, mice were placed in two separate chambers, one receiving a steady supply of high efficiency particulate (HEPA) filtered air, while the other chamber received air containing the concentrated ambient particles (CAPs)... All animals were exposed six hours daily for various amounts of time (9 days, 15 days or 21 days). During non-exposure hours, the animals were housed in normal cages (5 per cage) and were supplied with food and water ad libitum. After the final 6hr of exposure, the mice were euthanized by injecting sodium pentobarbital of 200 mg/kg into the peritoneal cavity. When unresponsive, the chest and abdominal cavity were exposed and blood was withdrawn directly from the heart using a 20-gauge hypodermic needle and syringe coated with 0.5 M ethylenediaminetetraacetic acid (EDTA)s. Additionally, the femur and tibia from both hind limbs were extracted, all skeletal muscle tissue was completely removed using dissecting scissors and tweezers, and the bones were flushed thoroughly with cold 1X phosphate buffer saline (PBS) to extract crude bone marrow cells to be used in further experiments. Some other organs (heart, lungs, liver, spleen) were collected and cryopreserved for future utilization.

## MONOUCLEAR CELL ISOLATION AND BONE MARROW CELLS

Whole blood extracted from the mice hearts was mixed with equal volume of 1X PBS and layered atop Ficoll solution and then centrifuged at 400G for 40 minutes. At the end of the spin, the buffy coat was collected, and centrifuged at 1200 rpm for 10 min.

The cell pellet was resuspended in 1ml PBS and a cell count was obtained using a BioRad Automated Cell Counter. The cell pellet was then divided up into 3 aliquots and re-centrifuged. The final, washed pellets were used for further assays, including, measurement of telomere length via Real Time PCR (RT-PCR), measurement of β-galactosidase activity by flow cytometry and assessment of histone methylation patterns via western blot.

After flushing in PBS, the crude bone marrow cells were centrifuged at 400G for 10 minutes and the supernatant was removed. The pelleted cells were washed once more with 1X PBS, resuspended and a cell count was obtained. From the 9 days exposure, half of the cells were used to culture endothelial progenitor cells (EPCs) which were harvested after 10 days and DNA was extracted from the harvested EPCs to measure telomere length via RT-PCR. The remaining half of the crude bone marrow flushed cells was used to magnetically sort ckit+ cells which were washed, and had DNA extracted from them to also measure telomere length via RT-PCR. From the 15 days exposure, half of the crude bone marrow cells were used to culture endothelial progenitor cells (EPCs) while the remaining cells were used to measure telomere length and histone methylation patterns via western blots. Finally, from the 21 days exposure the crude bone marrow cells were used directly in flow cytometry to measure cell senescence (β-gal activity) in bone marrow stem cells and stromal cells.

## CELL CULTURE

To culture EPCs, crude bone marrow cells were resuspended in EBM-2 basal media (Lonza, cat. no. CC-3156) containing EGMTM-2 SinglQuots® supplements (Lonza, cat. no. CC-4176) and 50 mL of fetal bovine serum. and plated onto a well in a 6 well fibronectin-coated plate (Corning, cat. no. 354402). An additional 3 mL of media was added onto each well containing cells, and the plates were placed in a sterile incubator with the temperature set to 37˚C and CO2 levels set at 5%. The media was changed out every 48 hours and once the cells reached 70-80% confluency (about 6-7 days), they were trypsinized using t 0.25% Trypsin-EDTA 1X (Gibco, cat. no. 25200-056) and re-plated in 100 mm Fibronectin coated dishes (Corning, cat. no. 354451). The cells were allowed to attach in individual 100 mm dishes for maximum yield and were cultured until confluent (typically 10-14 days after initial bone marrow flush). At this time, the cells were harvested, counted and aliquots were used for β-Gal activity assay, DNA isolation, histone extraction, and nuclear and cytoplasmic fractions extraction.

## REAL TIME PCR (TELOMERE LENGTH ASSESSMENT)

DNA was isolated using the Wizard®SV genomic DNA purification system kit (catalog no. A2360) from Promega and concentrations were obtained using a Nanodrop One spectrophotometer from Thermo Scientific. Real-time polymerase chain reaction assay was then performed on the DNA samples to measure an average telomere length using specific primers (forward: CCG TTT GTT TGG GTT TGG GTT TGG GTT TGG GTT TGG GTT; reverse: 5’ GGC TTG CCT TAC CCT TAC CCT TAC CCT TAC CCT TAC CCT ).The abundance of a single copy gene, acidic ribosomal phosphoprotein (36B4), was also determined by PCR with specific primers (forward:’ ACT GGT CTA GGA CCC GAG AAG 3; reverse: TCA ATG GTG CCT CTG GAG ATT) . Each reaction for telomeres consisted of 17.5 µL of Syber Green PCR Master Mix (QIAGEN cat. no.

330521), 300 nM each of the forward and the reverse primers, 35 ng of mouse DNA and enough DNAse free water to yield a 35 µL reaction mixture. Three 10ul samples of each mouse DNA were pipeted into adjacent wells as triplicates onto a 384 well PCR plate. An automated thermocycler (Quant Studio 5, Applied Biosystems) was used this analysis and the reaction conditions were set at 95 ˚C for 10 minutes, followed by 30 cycles of data collection at 95 ˚C for 15 seconds and an anneal-extend step at 56 ˚C for 1 minute. The 36B4 PCR assay consisted of 17.5 µL of Syber Green PCR Master Mix, 300 nM each of the forward and the reverse primers, and 70 ng of mouse DNA and enough DNAse free water to yield a 35 µL reaction mixture. The thermocycler reaction conditions were set at 95 ˚C for 10 minutes, followed by 35 cycles of data collection at 95 ˚C for 15 seconds, 56 ˚C for 20 seconds for annealing and 72 ˚C for 30 seconds for extension. To generate a standard curve normal mouse genomic DNA (Promega) was serially diluted over a 7-fold range for the telomere portion of the PCR, from 1.5 ng to 96.8 ng and for the 36B4 portion of the PCR from 3.27 to 118 ng per well. These standards were amplified as above. he Real-time PCR results were exported into an Excel Spreadsheet for analysis. Standard curves were generated using the Ct values and their corresponding log of DNA amount values. This standard curve was then used with the Ct values obtained from each well to calculate the amount of telomeric or 36B4 DNA for each mouse sample. The relative amount of telomeric DNA was then divided by its corresponding amount of 36B4 DNA to calculate the ratio of the telomere:36B4 to report as the average telomere length ratio.

Across all PCR results, the data was analyzed using excel spreadsheets and the telomere:36B4 ratios calculated were exported to Graphpad Prism to generate graphic representation of the data and to generate standard errors and p value to conclude if the differences between the two groups was statistically significant.

## β-GALACTOSIDASE ACTIVITY ASSAY

Other cell pellets (1.0 X $10^6$ cells/mL) were used for β-gal assay. These cells were fixed in 2% paraformaldehyde Thermo Scientific (Ref. no. 28906). by incubation for 10 minutes at room temperature protected from light. After the incubation, the cells were washed in 1% BSA in PBS to remove the fixation solution and then resuspended in 100µL of working solution. The working solution was prepared by dilution of the CellEvent Senescence Green Probe (1000X) into the pre-warmed CellEvent Senescence Buffer (1:250), both of which were components of the CellEventTM Senescence Green Detection Kit from ThermoFisher Scientific (Cat. no. C10850). After resuspension of the cells in the 100µL working solution, the tubes were incubated overnight (12 hours) at 37˚C after which the cells were washed once more with 1% BSA in PBS and resuspended in 300µL of 1% BSA in PBS and then analyzed on a Cytek Aurora, flow cytometer.

To analyze senescence in distinct bone marrow cell populations, after incubation with the working solution, the crude bone marrow cell mixture was washed once with 1% BSA in PBS and incubated with 5µL of mouse Fc block for 10 minutes at 4˚C. Then the cells were incubated with mixture of antibodies specific for stem cells (Alexa Fluor® 647 anti-mouse Ly-6A/E (Sca-1) (BioLegend cat.no. 122518; BV605 Rat Anti-Mouse CD34 (BD Biosciences cat.no. 750918)), or stromal cells. (Brilliant Violet 421TM anti-mouse CD73 (BioLegend cat.no.127217), APC/FireTM 750 anti-mouse CD105 (BioLegend cat.no. 120426), Brilliant Violet 750TM anti mouse CD45 (BioLegend cat.no. 103157)), was and incubated for 30 minutes protected from light at room temperature. After the incubation, the cells were washed with 300µL of 1% BSA in PBS and then resuspended in fresh 300µL of 1% BSA in PBS and analyzed on the Cytek Aurora. All flow files were exported and gating and analysis was accomplished using using FlowJo software. The

median fluorescence intensity was divided by the total β-Gal positive cells to give a normalized value for each mouse sample and this normalized data was entered into Graphpad Prism to generate graphical representations of the data, standard errors for each data population and a p value to determine if the differences were statistically significant.

## HISTONE EXTRACTION AND WESTERN BLOT

Histones were isolated from cell pellets using a histone extraction kit from Abcam (Cat. no. ab113476). In brief, the cells were suspended in 1X pre-lysis buffer (and incubates for 10 min on ice 10 minutes with gentle mixing. The cell lysates were then centrifuged at 10,000 rpm for 1 minute at 4˚C. The supernatant was removed and the cell pellet was resuspended in Lysis buffer and incubated on ice for 30 minutes. After the 30-minutes incubation, the tubes were centrifuged at 12,000 rpm for 5 minutes at 4˚C. The supernatant fraction was transferred to a new vial and Balance-DTT Buffer was added to the supernatant fraction immediately. The Balance-Dithiothreitol (DTT) buffer was made by adding 1 µL of DTT solution to 500 µL of the Balance Buffer. The protein concentration of the histone fractions was then quantified

Proteins were separated by polyacrylamide gel electrophoresis using 12% gels. 10 µg samples of the histone isolations were mixed with equal volume of 2X reducing buffer, heated at 100˚C for 5 minutes, cooled by placing vials in ice, and then loaded into the designated wells. A constant current of 60 milliAmps was used to separate the proteins. The proteins were then transferred to nitrocellulose membranes at a constant voltage of 100V for 1 hour after which the nitrocellulose membrane (BioRad, cat. no. 1620167) was blocked for 45 minutes in a 5% milk solution made by adding 2 g of non-fat dry blotting grade milk powder (BioRad cat.no. 170-6404) to 40 mL of 1X TBS solution. After blocking, primary was antibodies were added (1:1000) and the blots

were left to shake on an automated rocker over night at 4˚C. Each primary antibody was added on separate blots and the antibodies consist of H3K4me3 (Active Motif, cat. no. 39060), H3K9me3 (Cell Signaling Technology, cat. no. 4473S), H4K20 (Cell Signaling Technology, cat. no. 5737S). After primary antibody incubation, the blots were washed 3 times with TBST (50 mL of 10X TBS, 500 mL of distilled water, 1.65 mL of Tween®20 (MP Biomedicals, Cat. no. TWEEN201)). The secondary antibody (Anti-rabbit IgG, HRP-linked antibody, Cell Signaling Technology cat. no. 7074P2) was then added onto the blots at a dilution of 1:2000 with milk blocking solution and allowed to incubate on an automated rocker for 2 hours at room temperature. After this incubation, the secondary antibody was removed and the blots were washed 3 times with TBST. ClarityTM Western ECL Substrate solution (Cat. no.170-5061) was used to develop the blots. The solution was added onto the blots and allowed to incubate for 5 minutes before the image was developed by a ChemiDoc XRS+ molecular imager from BioRad. The developed images were exported in jpeg format and analyzed using the software ImageJ to quantify the band intensities. The blots were then stripped using RestoreTM Western Blot Stripping Buffer (Thermo Scientific, Cat. no. 21059). and the blots were washed 3 times with TBST before being blocked with 5% milk blocking solution for 45 minutes. Once the blocking was complete, the blots were incubated with antibodies recognized unmodified histone H3 or H4 antibody was added at a dilution of 1:1000. This was done to normalize the histone methylation blots to total histone protein. The remainder of the blotting procedure is as described above.

## NUCLEAR AND CYTOPLASMIC FRACTIONS EXTRACTION AND WESTERN BLOT

Nuclear and cytoplasmic fractions were extracted from EPCs using the NE-PER Nuclear and cytoplasmic extraction® kit from ThermoScientific (Cat. no. 78833 and

78835). The cytoplasmic extraction reagents were added first to separate the cytoplasmic fractions and pellet out the nuclei which had the nuclear extraction reagents added second to extract the nuclear fractions.

Proteins were separated by polyacrylamide gel electrophoresis using 10% gels. 50 µg samples of the cytoplasmic and nuclear fractions were mixed with equal volumes of 2X reducing buffer, heated at 100˚C for 5 minutes, cooled by placing vials in ice, and then loaded into the designated wells. A constant current of 60 milliAmps was used to separate the proteins. The proteins were then transferred to PVDF membranes (BioRad, cat. no. 1620177) at a constant voltage of 100V overnight after which the PVDF membrane was blocked for 45 minutes in a 5% milk solution made by adding 2 g of non-fat dry blotting grade milk powder (BioRad cat.no. 170-6404) to 40 mL of 1X TBS solution. After blocking, the primary antibody for mTERT, n was added (1:1000) and the blots were left to shake on an automated rocker over night at 4˚C. In addition, to verify the purity of the fractions, blots were incubated with antibodies for a nuclear antigen (lamin) and a cytoplasmic antigen (GAPDH). After primary antibody incubation, the blots were washed 3 times with TBST (50 mL of 10X TBS, 500 mL of distilled water, 1.65 mL of Tween®20 (MP Biomedicals, Cat. no. TWEEN201)). The secondary antibody (Anti-rabbit IgG, HRP-linked antibody, Cell Signaling Technology cat. no. 7074P2) was then added onto the blots at a dilution of 1:2000 with milk blocking solution and allowed to incubate on a rocker for 2 hours at room temperature. After this incubation, the secondary antibody was removed and the blots were washed 3 times with TBST. ClarityTM Western ECL Substrate solution (Cat. no.170-5061) was used to develop the blots. The solution was added onto the blots and allowed to incubate for 5 minutes before the image was developed by a ChemiDoc XRS+ molecular imager from BioRad.

The developed images were exported in jpeg format and analyzed using the software ImageJ to quantify the band intensities.

# RESULTS

## CAPS EXPOSURE $PM_{2.5}$ LEVELS

The data for our results was generated over several exposures. Average $PM_{2.5}$ levels across all exposures were between 74 μg/m3 to 86 μg/m3 with an enrichment factor ranging between 7 to 10 as shown in table 2.

| Exposures no. | Length of exposure | Average $PM_{2.5}$ levels ($\mu g/m^3$) | Enrichment Factor | No. of animals |
|---|---|---|---|---|
| 1 | 9 days | 84.72 | 7.87 | 10 |
| 2 | 9 days | 85.37 | 7.62 | 10 |
| 3 | 9 days | 79.79 | 10.00 | 10 |
| 4 | 15 days | 74.03 | 8.63 | 20 |
| 5 | 21 days | 78.28 | 10.00 | 15 |

**Table 2. $PM_{2.5}$ exposures summary**. Data table displaying exposure length, average $PM_{2.5}$ levels, enrichment factor and no. of animals for each individual exposure.

## TELOMERE LENGTH ASSESSMENT

Real time PCR was used to evaluate tel:scg ratio on DNA samples isolated from mice exposed to HEPA filtered air and CAPS. Results are depicted in Figure 1 and are from exposures of different lengths and PM concentrations (Table 2). They consistently show that telomere lengths decreased in bone marrow ckit positive (ckit+) cells, endothelial progenitor cells (EPC), mononuclear cells (MNC) and crude bone marrow cells in CAPS-exposed mice. In addition to the observed decrease across the multiple cell types, telomere length was measured in EPC in exposures of 3 different lengths (9

days, 15 days and 21 days) and the trend shows that with longer exposures the decrease in telomere length becomes more pronounced, even though the average $PM_{2.5}$ levels were approximately the same amount across all exposures as reported in Table 2. The mean decreases in tel:scg ratio of the CAPS air exposed mice compared to the HEPA filtered air exposed mice was also calculated for EPCs from the 9-,15-, and 21-days exposure and they were found to be 34.49%, 53.91% and 78.58% decrease respectively further proving that telomere attrition becomes more significant with longer exposures.

Additionally, the decrease in mean tel:scg ratios of the CAPS exposed mice compared to the HEPA filtered air exposed mice for the other cell types include an 81.97% decrease in ckit+ cells. Crude bone marrow cells were reported to show a 64.46% decrease in CAPS, and finally mononuclear cells showed a 34.49% decrease in CAPS exposed mice.

All bar graphs and statistical analyses was generated using the Graphpad prism software. Student's unpaired t-test was conducted to determine if difference in tel:scg ratios between HEPA filtered air and CAPS air exposed groups were statistically significant and across all exposures and cell types it was observed that the p value was less than 0.05 indicating that observed difference was statistically significant. Detailed individual p values for each comparison is reported in the figure legend of figure 1.

**RT-PCR results across all cell types experimented upon and across all exposures consistently showed a decrease in telomere length in CAPS exposed mice samples.**

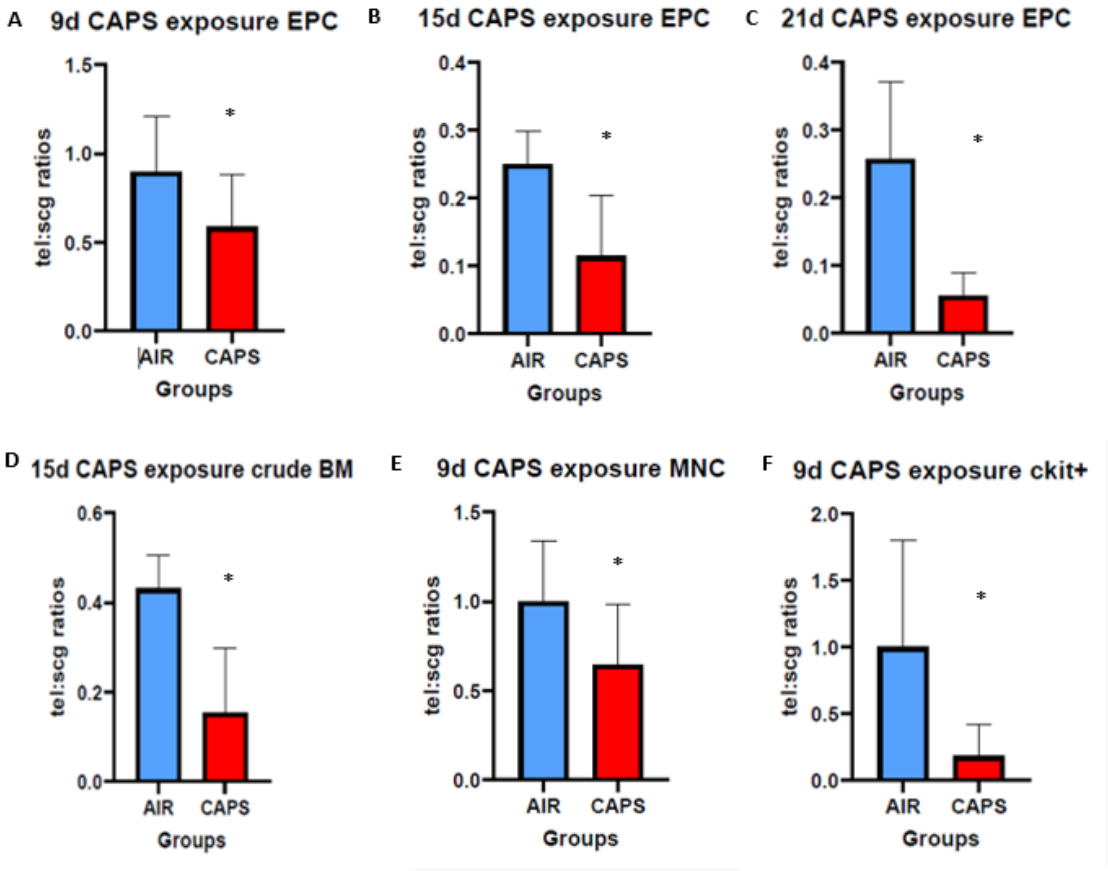


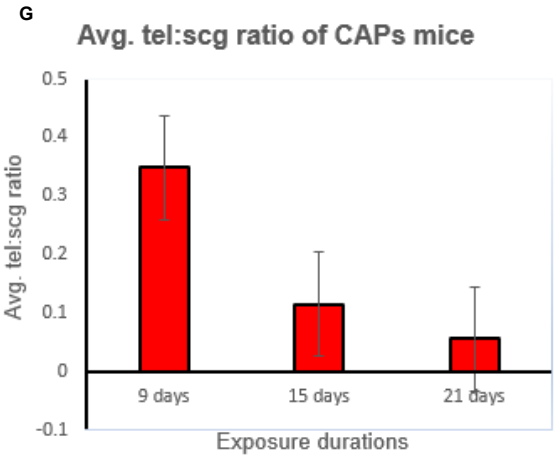


**Figure 1.** Telomere length assessment results. Illustrated are Bar graphs displaying tel:scg ratios in multiple cell types isolated from HEPA filtered air and CAPS exposed mice. Mouse samples were extracted from 5 different exposures, three of which were 9 days in length and the remaining being 15 days and 21 days. **A.** PCR results from 9 days exposure on cultured endothelial progenitor cells. p value 0.0094 *; **B.** PCR results from 15 days exposure on cultured endothelial progenitor cells. p value 0.0319 *; **C.** PCR results from 21 days exposure on cultured endothelial progenitor cells. p value 0.0116 *; **D.** PCR results from 15 days exposure on crude bone marrow cells. p value 0.0420 *; **E.** PCR results from 9 days exposure on peripheral blood mononuclear cells. p value 0.0403 *; **F.** PCR results from 9 days exposure on bone marrow ckit+ cells. p value 0.0220 *. **G.** Exposure duration response curve showing average $PM_{2.5}$ levels during each exposure and percentage telomere decrease in CAPs exposed groups.

## β-GALACTOSIDASE ACTIVITY MEASUREMENT

Higher amounts of β-Galactosidase activity indicate that there was greater senescence. This was determined in several cell types from Air- and CAPS- exposed mice including peripheral blood mononuclear cells, endothelial progenitor cells, bone marrow stromal cells and bone marrow stem cells. Across all cell types β-Galactosidase activity was increased in the samples from mice that were exposed to CAPS (Figure 2). Thus $PM_{2.5}$ induces cell senescence.

The greater increase in β-Galactosidase activity was observed in bone marrow stromal cells in CAPS exposed mice (Fig. 2 C) indicating a defective bone marrow microenvironment. The average increase in β-Galactosidase activity was calculated to be 91.15% in CAPS exposed mice indicating a significantly high amount of cellular senescence upon exposure to $PM_{2.5}$ compared to the bone marrow stem cells which showed an increase of 71.93%. The calculated β-Galactosidase activity increase in mononuclear cells was found to be 72.22%, which was almost if not slightly higher than the stem cells. Endothelial progenitor cells showed the lowest amount of β-Galactosidase activity indicating the overall senescence levels in these cells were the lowest observed among the three cell types.

Since bone marrow stromal cells play an important role in regulating hematopoietic stem and progenitor cells by providing cytokines and growth factors there is the potential that a defective bone marrow microenvironment can give rise to hematological malignancies and development of bone marrow diseases, such as myeloproliferative-like diseases, myelodysplastic syndrome or leukemia [38]. It is also important to note that bone marrow stem cells can differentiate into several different types of blood cells, high levels of senescence in these cells can be problematic and lead to blood related diseases such as leukemia, aplastic anemia, lymphoma, etc. [39]

Endothelial progenitor cells are circulating cells, that adhere to the endothelium at sites of hypoxia or ischemia, and play an important role in new vessel formation [40]. They are critical in the repair and regeneration of damaged blood vessel, hence senescence in EPCs can limit their number or endothelial function. Not only that, senescent EPCs can further induce failure of angiogenesis since these cells do not respond to mitogenic stimuli and may potentially increase risk of atherosclerosis [41] which is why it was important to investigate senescence levels in EPCs.

Since mononuclear cells are critical components of the innate and adaptive immune systems which defend the body against viral, bacterial, and parasitic infections; as well as destroys tumor cells and foreign substances, it was important that we investigate the senescence levels in this type of cell as well. The observed senescence in this kind of cells may lead to a decreased ability to fight infections and thereby contribute to progression of diseases [42]. Mononuclear cells include any blood cell with a round nucleus such as lymphocytes, monocytes, natural killer cells or dendritic cells [40]. The β-Galactosidase activity assay in MNCs was used to look at the overall levels of senescence and not any specific cell mononuclear cell type. In future experiments we may attempt to identify the senescence levels in specific mononuclear types using antigen-specific antibodies in the flow cytometry assay.

All bar graphs and statistical analyses was generated using the Graphpad prism software. Student's unpaired t-test was conducted to determine if difference in β-galactosidase activity per cell type between HEPA filtered and CAPS air exposed groups were statistically significant and across all exposures and cell types it was observed that the p value was less than 0.05 indicating that observed difference was statistically significant. Detailed individual p values for each comparison is included in the figure legend of figure 2. **Mice exposed to CAPS displayed higher levels of β-**

**Galactosidase activity compared to control mice which were exposed to HEPA filtered air. A flow cytometry-based B-gal assay was used to assess the level of senescence.**

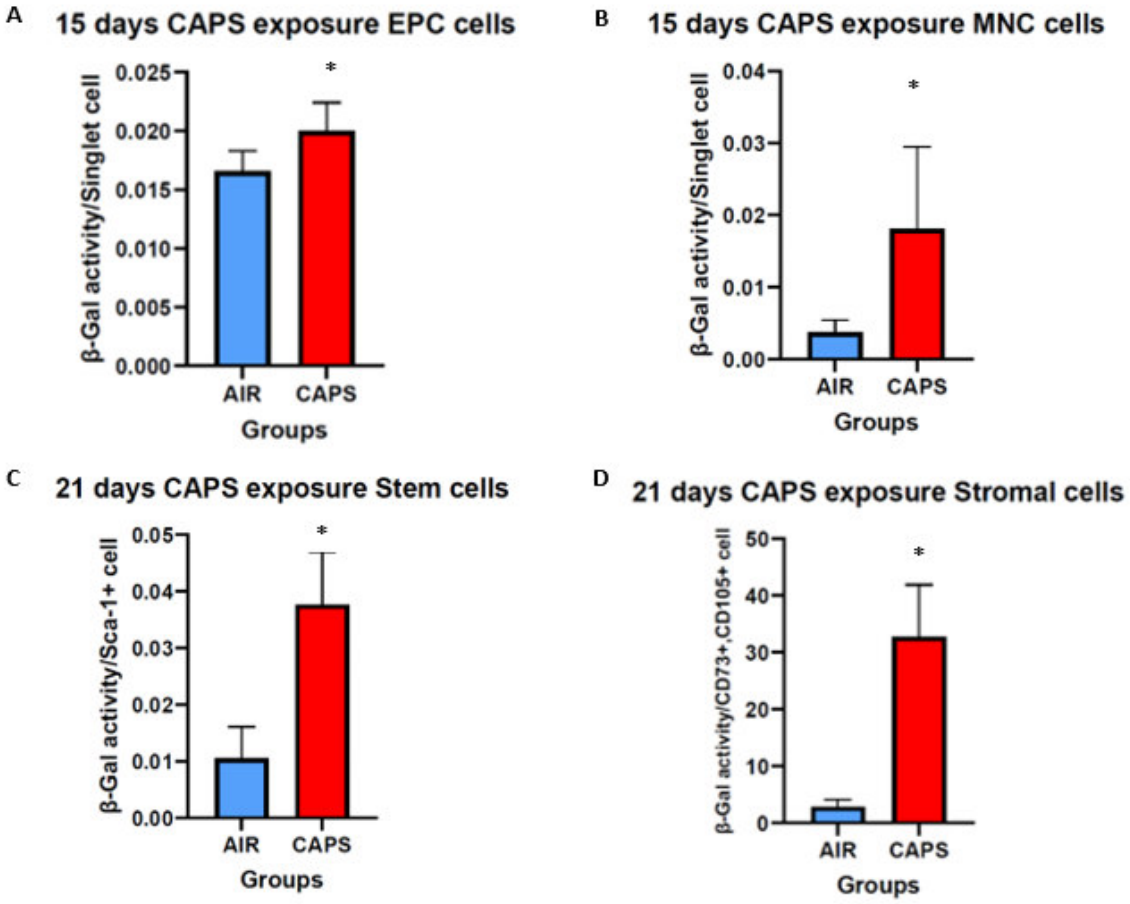


**Figure 2.** Flow associated β-galactosidase activity assay results. Bar graphs demonstrating levels of β-Galactosidase activity across multiple cell types in CAPS (red) and HEPA filtered air (blue) exposed mice.
**A.** 15 days exposure EPC cells, p value 0.0340 *; **B.** 15 days exposure MNC cells, p value 0.0235 *; **C.** 21 days exposure bone marrow stem cells, p value <0.0001 *; **D.** 21 days exposure bone marrow stromal cells, p value <0.0001 *.

## HISTONE METHYLATION LEVELS ASSESSMENT

As mentioned previously H3K4me3 and H4K20me3 levels increase with age and H3K9me3 levels decrease with age. In our experiments H3K4me3 was investigated in histones extracted from MNCs and EPCs and in both cases an increased level of

H3K4me3 level was observed indicating that accelerated aging has occurred in CAPS air exposed mice (Figs. 3 A, B, C, D, I, J). The average increase in H3K4me3 level in CAPS exposed mice was calculated to be 22.12% in MNCs and 49.18% in EPC. Additionally, the 2 other histone methylation levels H3K9me3 and H4K20me3 was investigated in EPCs and was observed to decrease (55.25%) and increase (25.45%) respectively in CAPS air exposed mice (Figs. E, F, G, H, K, L), indicating that $PM_{2.5}$ exposure can cause premature aging. All bar graphs and statistical analyses was generated using the Graphpad prism software. Student's unpaired t-test was conducted to determine if the differences in the observed H3K4me3, H3K9me3 and H4K20me3 levels per cell type between HEPA filtered and CAPS air exposed groups were statistically significant, and across all exposures and cell types it was observed that the p value was less than 0.05 indicating that observed difference was statistically significant. Detailed individual p values for each comparison is included in the figure legend of figure 3. MNC histone yield was not high enough to investigate the other 2 histone methylation patterns which were investigated in EPCs. Future experiments to investigate the levels of H3K9me3 and H4K20me3 will need to be conducted in MNCs.

Thus, in addition to telomere shortening and cellular senescence MNCs and EPCs from CAPS-exposed mice also displayed this age-related epigenetic modification. This may result in altered gene expression and cellular function. There are several human diseases and adverse responses arising from exposure to environmental chemicals that are associated with aberrant histone methylation patterns and increased risks of cancers, neurological disorders, diabetes and increased inflammation [38, 43].

Western blots performed to observe epigenetic changes in mononuclear and endothelial progenitor cells' histones showed the same trends as aging, indicating that accelerated aging has occurred in CAPS exposed mice.

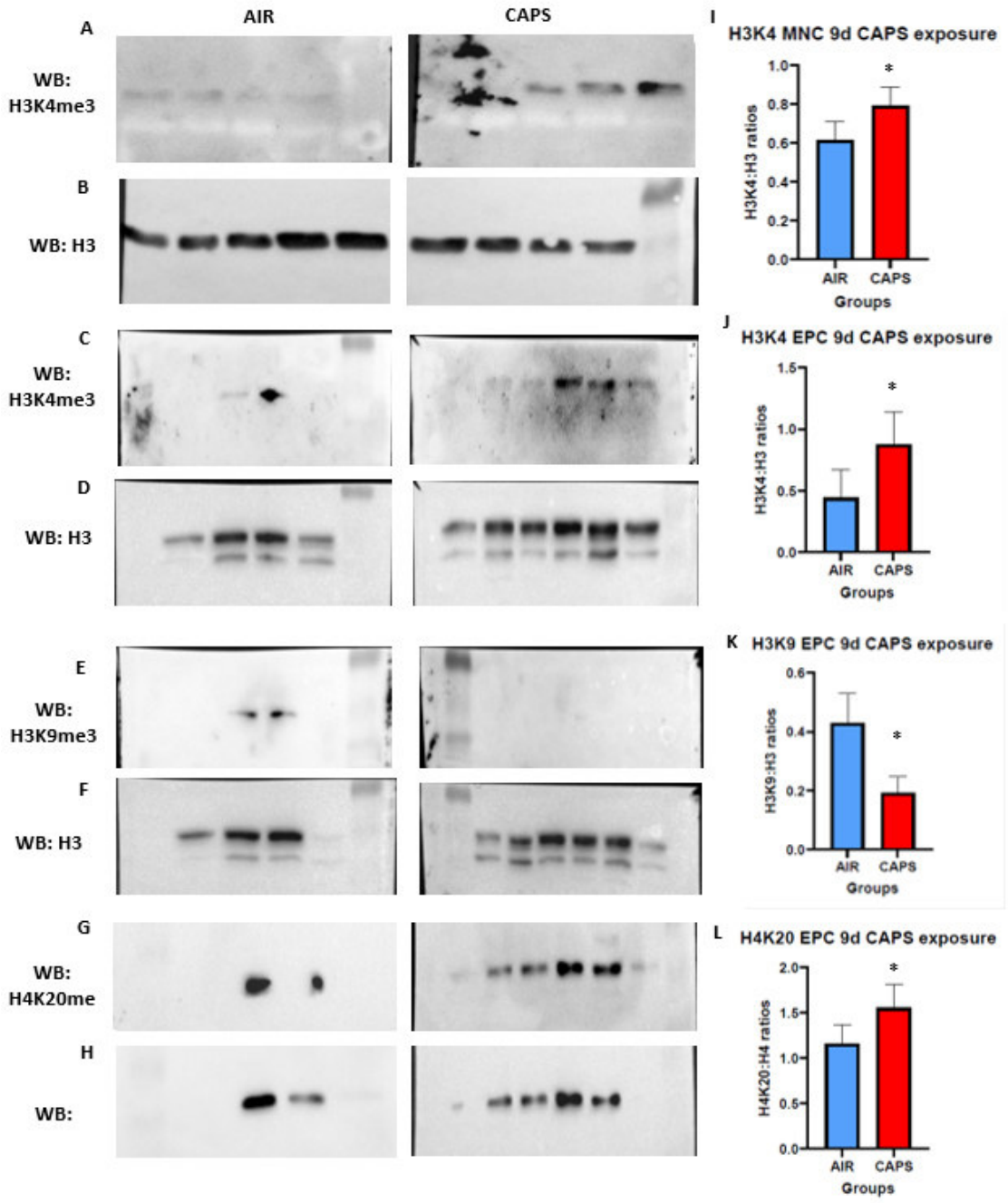


**Figure 3.** Histone methylation Western blots with quantification graphs. Western blots displaying histone methylation levels in mice exposed to HEPA filtered air and CAPS for 9 days. All blots on the left are AIR samples and all on the right are CAPS samples. Each row of blots was probed with the same antibody.
**A.** Western blot showing protein bands for H3K4me3 at 17 kDa (MNC); **B.** Western blot showing protein bands for H3 at 15kDa (MNC); **C.** Western blot showing protein bands for H3K4me3 at 17 kDa (EPC); **D.** Western blot showing protein bands for H3 at 15kDa (EPC); **E.** Western blot showing protein bands for H3K9me3 at 13 kDa (EPC); **F.** Western blot showing protein bands for H3 at 15 kDa (EPC); **G.** Western blot showing protein bands for H4K20me3 at 8 kDa (EPC); **H.** Western blot showing protein bands for H4 at 14 kDa

(EPC); **I.** Bar graph showing quantified H3K4me3 levels in HEPA filtered air vs CAPS air exposed mouse MNCs normalized to total histone protein H3, p value 0.0383 *; **J.** Bar graph showing quantified H3K4me3 levels in HEPA filtered air vs. CAPS air exposed mouse EPCs normalized to total histone protein H3, p value 0.0292 *; **K.** Bar graph showing quantified H3K9me3 levels in HEPA filtered air vs. CAPS air exposed mouse EPCs normalized to total histone protein H3, p value 0.0012 *; **L.** Bar graph showing quantified H4K20me3 levels in HEPA filtered air vs. CAPS air exposed mouse EPCs normalized to total histone protein H4, p value 0.0413 *.

## MOUSE TELOMERASE LOCALIZATION DETECTION

As mentioned above, Y 707 on hTERT is conserved in mTERT. This residue is phosphorylated by c-Src protein which in turn can be activated by $PM_{2.5}$ exposure [18]. This TERT modification would hypothetically result in the egress of TERT from the nucleus. However, when we looked at this possibility in EPC extracts from 9-day exposure mice, we observed that there was no increase in cytoplasmic TERT, indicating that exposure to $PM_{2.5}$ did not cause the egress of mTERT from the nucleus as shown by the graphical representation in Fig. 4 C. After quantification of the bands it can clearly be seen that the levels of mTERT were higher in the nuclear fractions of both HEPA filtered air and CAPS exposed groups compared to the levels in the cytoplasmic fractions. If we calculate the averages of all the groups, we can see a very small decrease in the nuclear fraction of the CAPS group compared to the nuclear fraction of the AIR group, but this difference was deemed to be statistically insignificant after conducting the unpaired student's T-test. Thus, telomere attrition resulting from exposure to $PM_{2.5}$ is being caused by some other mechanism, yet to be identified. Nevertheless, we will test this idea in other cell types such as the MNCs and bone marrow ckit+ cells, which also show telomere attrition upon exposure. In EPCs $PM_{2.5}$ exposure does not cause nuclear egress of mTERT from the and hence cannot be considered as a possible mechanism behind telomere attrition in $PM_{2.5}$ exposed mice.

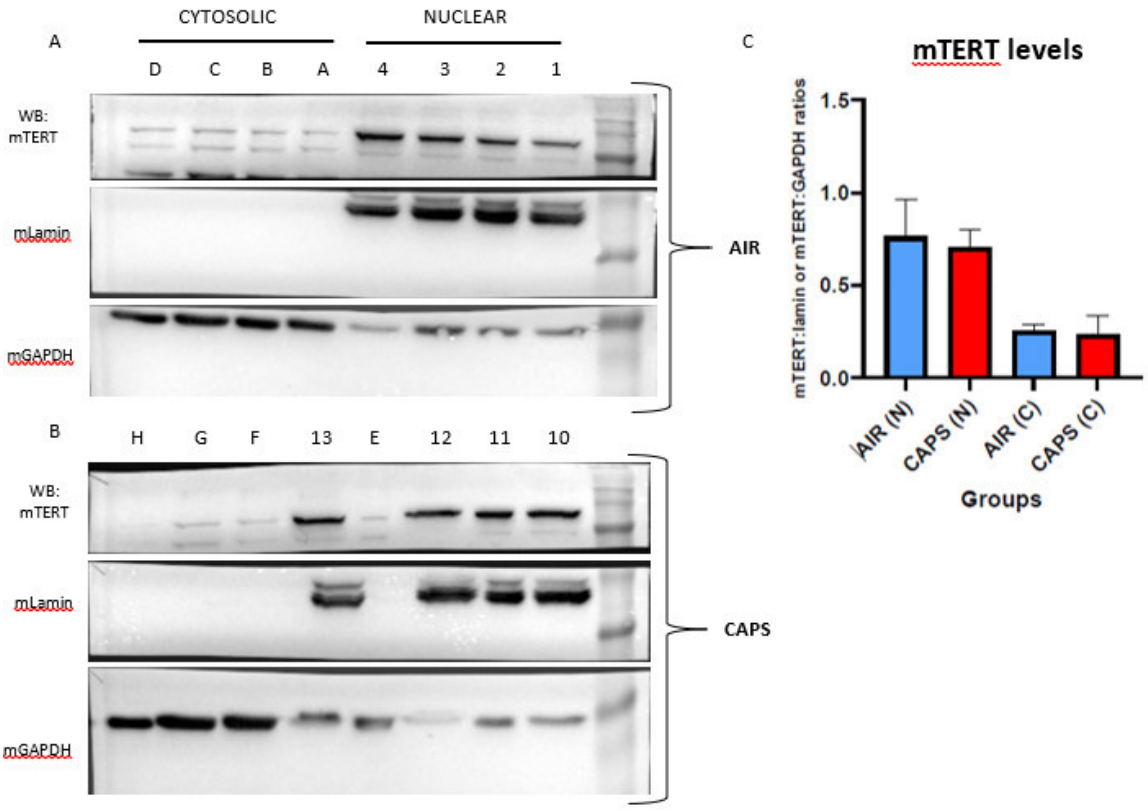


**Figure 4. mTERT localization western blots with quantification graphs**. Western blots with quantified bar graphs displaying the levels of mTERT in nuclear and cytosolic fractions in 9-days CAPS exposed EPCs.

**A.** Western blots showing protein bands of mTERT at 127 kDa, mLamin at 74 kDa and mGAPDH at 36 kDa in HEPA filtered air exposed samples. Samples in lanes 1-4 from the right are all nuclear fractions as indicated by the labels in figures while the remaining samples A-D are their respective cytosolic fractions. **B.** Western blots showing protein bands of mTERT at 127 kDa, mLamin at 74 kDa and mGAPDH at 36 kDa in CAPS exposed samples. Samples from 10-13 are nuclear fractions while the samples denoted by the letter E-H are their respective cytosolic fractions. **C.** Bar graph displaying the quantified levels of mTERT in the nuclear and cytosolic fractions for HEPA filtered air and CAPS exposed mouse EPC. P value AIR(N) vs CAPS(N) was 0.6292, ns. P value for AIR(C) vs CAPS(C) was 0.7570, ns.

## DISCUSSION

In this preliminary study, the effects of $PM_{2.5}$ on aging was investigated. Out of the 9 hallmarks of aging, this study focused on 3 which included telomere length measurement, cellular senescence and histone methylation patterns. In previous literature, it has been reported that telomere length decrease is a consequence of aging, followed by increased cellular senescence and changes in certain histone methylation patterns.

Typically, the effects of $PM_{2.5}$, or environmental exposures, on markers of aging have been studied using blood leukocytes. A novel feature of this study was the use of multiple cell types to determine the breadth and extent of $PM_{2.5}$-mediated effects. Thus, we measured hallmarks of aging on three cell types, including bone marrow ckit positive (ckit+) cells, endothelial progenitor cells (EPC) cultured from flushed bone marrow, and peripheral blood mononuclear cells (PBMNC). We found that, after 9-day of CAPS exposure, telomere lengths were significantly decreased in all three cell types.

Bone marrow ckit+ cells are progenitor cells that have been shown to differentiate into multiple cell types, including cardiomyocytes, endothelial cells and vascular smooth muscle cells. Treatment with these cells can reduce the size of myocardial infarction scars and maintain the left ventricle ejection function and are considered to be the primary factors driving myocardium regeneration following myocardial infarction [44]. Since these cells are important functional cells we were interested to see if they undergo telomere attrition as a consequence of getting exposed to $PM_{2.5}$, and as our RT-PCR

results show, they were among the cell types that showed the highest decrease in telomere length upon $PM_{2.5}$ exposure (Fig. 1F).

A second cell type are EPCs. These are bone marrow-resident stem cells that are recruited into circulation and to the endothelium at sites of injury. They also play a very important role in angiogenesis and are critical in the repair and regeneration of damaged blood vessels. Hence, telomere shortening and the subsequent cellular senescence in EPCs can be detrimental to the endothelial function [40]. In addition, senescent EPCs may have impaired function, since these cells do not respond to mitogenic stimuli and may potentially increase risk of atherosclerosis [41]. Our initial RT-PCR experiments on EPC from 9-day CAPS exposure showed a significant decrease in telomere length (Fig. 1A). When we performed additional exposures of 15- and 21-days, we observed that telomere attrition was not only maintained but a comparably larger decrease was observed with the increasing length of exposure. Previous literature mentions how telomere length decrease can lead to cellular senescence over time [9], hence, we also analyzed β-galactosidase activity on the EPC samples from the 15 days exposure. The results (Fig. 2A) indicates that there was marked increase in β-galactosidase activity indicating that the amount of cellular senescence was high in mice exposed to $PM_{2.5}$.

The third cell type that was investigated was MNCs mainly because this class of cells comprises immune response cells such as lymphocytes, monocytes, natural killer cells or dendritic cells [40]. These are cells that help to defend the body against viral, bacterial, and parasitic infections as well as destroy tumor cells and foreign substances [42]. Hence, if these cells undergo telomere length attrition, cell cycle arrest, and senescence, the body's chances of fighting and surviving infections decrease and it leaves individuals more prone to not just infectious diseases but also to cancers. Our

PCR results from the 9 days exposure show that there is a decrease in telomere length in MNC when exposed to $PM_{2.5}$ (Fig. 1E) and additional 15-day exposures showed that these cells also undergo senescence (Fig. 2B).

We also measured telomere lengths in crude bone marrow cells which were cells that were flushed with PBS directly from the femur and tibia and were not cultured (like EPCs) or magnetically separated (like the ckit+ cells). These cells also demonstrated a decrease in telomere length with $PM_{2.5}$ exposure (Fig. 1D). Since this crude bone marrow fraction contained stem cells and stromal cells, we also measured β-galactosidase activity in these discrete fractions using antibodies to characteristic surface antigens in a flow cytometry assay. The results of this analysis show that there was an increase in β-galactosidase activity in both stem cells and stromal cells, upon $PM_{2.5}$ exposure, and that the stromal cell fraction had a 19.22% higher activity than stem cell samples (Figs. 2C & D). This increased senescence in stromal cells is indicative of a defective bone marrow microenvironment and because these cells play such a crucial role in regulating hematopoietic stem and progenitor cells by providing cytokines and growth factors there is the potential that senescence in stromal cells can give rise to hematological malignancies and bone marrow diseases [38]. Additionally, like stromal cells, high levels of senescence in stem cells is also cause of concern since it can lead to blood related diseases such as leukemia, aplastic anemia and lymphoma [39].

In addition to the observations of telomere lengths decrease and increased cellular senescence in $PM_{2.5}$ exposed mice, we also observed changes in histone methylation patterns (H3K4me3, H3K9me3 and H4K20me3). Histone methylation patterns like these have often been used as biomarkers of aging, as H3K4me3 and H4K20me3 levels increase with age, while H3K9me3 levels decrease with age [30]. These histone methylations give rise to altered gene expression and have been

implicated in several diseases. One such example is that increased levels of H3K4me3 have been associated with an upregulation of inflammatory gene expression [45]. Studies have shown that exposure to heavy metals such as arsenic or mercury [46] and endocrine disrupting chemicals such as bisphenol A or organochlorines [47] can also cause alterations in histone methylation. In MNCs we observed that there was an increase of H3K4me3 upon $PM_{2.5}$ exposure giving us further proof of accelerated aging in these cells (Fig. 3A, I). When using EPCs in this analysis, we found that H3K4me3 and H4K20me3 levels were increased while H3K9me3 levels decreased with $PM_{2.5}$ exposure (Fig. 3C, E, G, J, K, L), consistent with aging patterns [29]. Since histone methylation can alter the gene expression patterns, it would be of interest to further investigate which genes are being downregulated or upregulated in these cell types which show the aging trend with $PM_{2.5}$ exposure. This will allow us to identify if these epigenetic alterations being observed as a consequence of $PM_{2.5}$ exposure can contribute to any potential diseases. In addition to gene expression levels, it would be important to investigate if changes in histone methylation occur in multiple cell types or are cell-type specific.

The results from these exposure studies provide ample evidence that accelerated aging is occurring in these mice that are being exposed to $PM_{2.5}$. While these markers (telomere attrition, cellular senescence, altered histone methylation patterns provide evidence of $PM_{2.5}$ associated aging, a mechanistic understanding is lacking. Our attempt to understand if the phosphorylation of tyrosine residue at site 707 by c-Src activation as a consequence of $PM_{2.5}$ exposure did not give us the expected results. It was observed as mentioned earlier that $PM_{2.5}$ exposure does not cause the activation of c-Src and thereby cause the phosphorylation of Y707, subsequently causing the egress of mTERT from the nucleus. However, this experiment was only

performed in one cell type and we cannot discard this idea fully without first investigating the other cell types. Telomere lengths are maintained not only by mTERT activity but also other proteins such as the Shelterin protein complex which is a 6-protein complex consisting of TRF1, TRF2, RAP1, POT1, TPP1 and TIN2. It helps in promoting the recruitment of telomerase and the addition of multiple telomeric repeats after the single substrate binding event during telomeric elongation [48]. Other experiments to consider would be TERT activity assays to compare the TERT activity levels in HEPA filtered air vs CAPS exposed mice across different cell types. Investigating along such paths in the future may provide a better understanding of how exposure to $PM_{2.5}$ is causing such rapid reduction in telomere ends and thereby causing premature cellular senescence. Future experiments investigating the activity of the telomerase enzyme or the expression levels of the Shelterin proteins can potentially provide us with not only understanding of the mechanism but also a target for possible treatments.

Furthermore, as mentioned previously senescent cells secrete pro-inflammatory factors known as senescence associated secretory phenotype (SASPs) which can contribute to the functional disruption of tissues in an autocrine or paracrine manner leading to the senescence of neighboring cells via immunosuppression and inflammation [21]. By understanding and targeting components of SASPs, rather than targeting individual diseases that are downstream of fundamental aging processes, it may be possible to reverse this premature aging effect of $PM_{2.5}$. One such way to reverse this would be via the use of senolytic drugs such as Dastnib, Quercetin, Fisetin or Navitoclax [49] to name a few. These drugs target senescent cells and lyse and clear them before the SASPs secreted by senescent cells can cause surrounding healthy cells to become senescent and increase the burden on immune cells like natural killer cells which can naturally clearing out senescent cells within days to weeks [50]. This can be a future

area of investigation to see if the consequences of premature aging caused by exposure to $PM_{2.5}$ can be successfully reversed via the use of senolytics and thereby prevent the development of age-related diseases.

REFERENCES


1. Meo, S.A., et al., *Effect of environmental air pollution on type 2 diabetes mellitus.* Eur Rev Med Pharmacol Sci, 2015. 19(1): p. 123-8.
2. Gold, D.R., et al., *Ambient pollution and heart rate variability.* Circulation, 2000. 101(11): p. 1267-73.
3. Lee, B.J., B. Kim, and K. Lee, *Air pollution exposure and cardiovascular disease.* Toxicol Res, 2014. 30(2): p. 71-5.
4. Yasukawa, M., et al., *CDK1 dependent phosphorylation of hTERT contributes to cancer progression.* Nat Commun, 2020. 11(1): p. 1557.
5. Huang, C.H., et al., *Detrimental correlation between air pollution with skin aging in Taiwan population.* Medicine (Baltimore), 2022. 101(31): p. e29380.
6. Chang-Chien, J., et al., *Particulate matter causes telomere shortening and increase in cellular senescence markers in human lung epithelial cells.* Ecotoxicol Environ Saf, 2021. 222: p. 112484.
7. Miri, M., et al., *Association of greenspace exposure with telomere length in preschool children.* Environ Pollut, 2020. 266(Pt 1): p. 115228.
8. Miri, M., et al., *Air pollution and telomere length in adults: A systematic review and meta-analysis of observational studies.* Environ Pollut, 2019. 244: p. 636-647.
9. López-Otín, C., et al., *The hallmarks of aging.* Cell, 2013. 153(6): p. 1194-217.

10. Bernadotte, A., V.M. Mikhelson, and I.M. Spivak, *Markers of cellular senescence. Telomere shortening as a marker of cellular senescence.* Aging (Albany NY), 2016. 8(1): p. 3-11.
11. Groten, J., A. Venkatraman, and R. Mertelsmann, *Modeling and Simulating Carcinogenesis*. 2018. p. 277-295.
12. Cohen, S.B., et al., *Protein composition of catalytically active human telomerase from immortal cells.* Science, 2007. 315(5820): p. 1850-3.
13. Bhattacharyya, J., et al., *Telomere length as a potential biomarker of coronary artery disease.* Indian J Med Res, 2017. 145(6): p. 730-737.
14. Shammas, M.A., *Telomeres, lifestyle, cancer, and aging.* Curr Opin Clin Nutr Metab Care, 2011. 14(1): p. 28-34.
15. Reichert, S. and A. Stier, *Does oxidative stress shorten telomeres in vivo? A review.* Biol Lett, 2017. 13(12).
16. Nishio, N. and S. Kojima, *Recent progress in dyskeratosis congenita.* Int J Hematol, 2010. 92(3): p. 419-24.
17. Chung, J., P. Khadka, and I.K. Chung, *Nuclear import of hTERT requires a bipartite nuclear localization signal and Akt-mediated phosphorylation.* J Cell Sci, 2012. 125(Pt 11): p. 2684-97.
18. Geraghty, P., A. Hardigan, and R.F. Foronjy, *Cigarette smoke activates the proto-oncogene c-src to promote airway inflammation and lung tissue destruction.* Am J Respir Cell Mol Biol, 2014. 50(3): p. 559-70.
19. Zhang, L., et al., *Cellular senescence: a key therapeutic target in aging and diseases.* J Clin Invest, 2022. 132(15).
20. Hayflick, L., *The future of ageing.* Nature, 2000. 408(6809): p. 267-9.
21. Birch, J. and J. Gil, *Senescence and the SASP: many therapeutic avenues.* Genes Dev, 2020. 34(23-24): p. 1565-1576.

22. Ho, C.Y. and O. Dreesen, *Faces of cellular senescence in skin aging.* Mech Ageing Dev, 2021. 198: p. 111525.

23. Vasileiou, P.V.S., et al., *Mitochondrial Homeostasis and Cellular Senescence.* Cells, 2019. 8(7).

24. Eckhart, L., E. Tschachler, and F. Gruber, *Autophagic Control of Skin Aging.* Front Cell Dev Biol, 2019. 7: p. 143.

25. Lee, Y.I., et al., *Cellular Senescence and Inflammaging in the Skin Microenvironment.* Int J Mol Sci, 2021. 22(8).

26. Davalli, P., et al., *ROS, Cell Senescence, and Novel Molecular Mechanisms in Aging and Age-Related Diseases.* Oxid Med Cell Longev, 2016. 2016: p. 3565127.

27. Jin, S., et al., *Antioxidants prevent particulate matter-induced senescence of lung fibroblasts.* Heliyon, 2023. 9(3): p. e14179.

28. Ryu, Y.S., et al., *Particulate matter-induced senescence of skin keratinocytes involves oxidative stress-dependent epigenetic modifications.* Exp Mol Med, 2019. 51(9): p. 1-14.

29. Albini, S., et al., *Epigenetic Reprogramming of Human Embryonic Stem Cells into Skeletal Muscle Cells and Generation of Contractile Myospheres.* Cell Reports, 2013. 3(3): p. 661-670.

30. Wang, K., et al., *Epigenetic regulation of aging: implications for interventions of aging and diseases.* Signal Transduct Target Ther, 2022. 7(1): p. 374.

31. Sun, D., et al., *Epigenomic profiling of young and aged HSCs reveals concerted changes during aging that reinforce self-renewal.* Cell Stem Cell, 2014. 14(5): p. 673-88.

32. Jeon, H.J., et al., *Effect of heterochromatin stability on intestinal stem cell aging in Drosophila.* Mech Ageing Dev, 2018. 173: p. 50-60.

33. Bonasio, R., S. Tu, and D. Reinberg, *Molecular signals of epigenetic states.* Science, 2010. 330(6004): p. 612-6.

34. Shumaker, D.K., et al., *Mutant nuclear lamin A leads to progressive alterations of epigenetic control in premature aging.* Proc Natl Acad Sci U S A, 2006. 103(23): p. 8703-8.

35. Baumgart, M., et al., *RNA-seq of the aging brain in the short-lived fish N. furzeri - conserved pathways and novel genes associated with neurogenesis.* Aging Cell, 2014. 13(6): p. 965-74.

36. Kronfol, M.M., et al., *DNA methylation and histone acetylation changes to cytochrome P450 2E1 regulation in normal aging and impact on rates of drug metabolism in the liver.* Geroscience, 2020. 42(3): p. 819-832.

37. Fraga, M.F. and M. Esteller, *Epigenetics and aging: the targets and the marks.* Trends Genet, 2007. 23(8): p. 413-8.

38. Li, H., et al., *Early growth response 1 regulates hematopoietic support and proliferation in human primary bone marrow stromal cells.* Haematologica, 2020. 105(5): p. 1206-1215.

39. Gronthos, S., et al., *A novel monoclonal antibody (STRO-3) identifies an isoform of tissue nonspecific alkaline phosphatase expressed by multipotent bone marrow stromal stem cells.* Stem Cells Dev, 2007. 16(6): p. 953-63.

40. Kleiveland, C.R., *Peripheral Blood Mononuclear Cells*, in *The Impact of Food Bioactives on Health: in vitro and ex vivo models*, K. Verhoeckx, et al., Editors. 2015, Springer

Copyright 2015, The Author(s). Cham (CH). p. 161-7.

41. Yoder, M.C., *Human endothelial progenitor cells.* Cold Spring Harb Perspect Med, 2012. 2(7): p. a006692.

42. Huang, W., et al., *Cellular senescence: the good, the bad and the unknown.* Nat Rev Nephrol, 2022. 18(10): p. 611-627.

43. Cui, J.Y., Z.D. Fu, and J. Dempsey, *Chapter 1-2 - The Role of Histone Methylation and Methyltransferases in Gene Regulation*, in *Toxicoepigenetics*, S.D. McCullough and D.C. Dolinoy, Editors. 2019, Academic Press. p. 31-84.

44. Li, C., et al., *c-kit Positive Cardiac Outgrowth Cells Demonstrate Better Ability for Cardiac Recovery Against Ischemic Myopathy.* J Stem Cell Res Ther, 2017. 7(10).

45. Li, Y., et al., *Role of the histone H3 lysine 4 methyltransferase, SET7/9, in the regulation of NF-kappaB-dependent inflammatory genes. Relevance to diabetes and inflammation.* J Biol Chem, 2008. 283(39): p. 26771-81.

46. Gadhia, S.R., A.R. Calabro, and F.A. Barile, *Trace metals alter DNA repair and histone modification pathways concurrently in mouse embryonic stem cells.* Toxicol Lett, 2012. 212(2): p. 169-79.

47. De Coster, S. and N. van Larebeke, *Endocrine-disrupting chemicals: associated disorders and mechanisms of action.* J Environ Public Health, 2012. 2012: p. 713696.

48. Mir, S.M., et al., *Shelterin Complex at Telomeres: Implications in Ageing.* Clin Interv Aging, 2020. 15: p. 827-839.

49. Kirkland, J.L. and T. Tchkonia, *Senolytic drugs: from discovery to translation.* J Intern Med, 2020. 288(5): p. 518-536.

50. Chaib, S., T. Tchkonia, and J.L. Kirkland, *Cellular senescence and senolytics: the path to the clinic.* Nat Med, 2022. 28(8): p. 1556-1568.

CURRICULUM VITAE

Daniel Gomes, B.A., Biochemistry
University of Louisville School of Medicine
Department of Pharmacology & Toxicology
302 E. Muhammad Ali Blvd. (CII, Rm 313)
Louisville, KY 40202
Phone: (502) 963-7876
E-mail: dcgome02@louisville.edu

---

## Education

| | |
|---|---|
| 2014 – 2018 | B.A., Biochemistry,<br>Earlham College, Richmond, IN |
| 2020 – Present | M.S./Ph.D., Pharmacology & Toxicology<br>University of Louisville, School of Medicine, Louisville, KY |

## Research Experience

| | |
|---|---|
| 2015 | Undergraduate Research Assistant<br>Earlham College, Department of Chemistry, Richmond, IN |
| 2016 | Summer student research intern<br>Indiana University–Purdue University Indianapolis, Dept. of Medicine, Herman B Wells Center for Pediatric Research, Indianapolis, IN |
| 2017 | Summer student research intern<br>University of Louisville, Department of Medicine, Diabetes and Obesity Center, Louisville, KY |
| 2018 -2020 | Research Technician I<br>University of Louisville, School of Medicine, Christina Lee Brown Envirome Institute, Louisville, KY |

## Other Experience and Professional Memberships

| | |
|---|---|
| 2021 – Present | Trainee, Superfund Research Program (SRP) |
| 2018 – Present | Member, Christina Lee Brown Envirome Institute |

## Honors and Awards

| | |
|---|---|
| 2014 | International Student Academic Scholarship |
| 2016 | Joseph Moore Museum Science Communication Award |
| 2016 | Earlham College Fall Semester Scholar Athlete Award |
| 2017 | DJ Angus Scientech Award |

## Presentations and Publications

### Presentations

1. Poster presentation, D. Gomes, O. Layne, C. Carter, J. Zhao, T.E. O'Toole. "PM2.5 exposure and the induction of accelerated aging in mice", Research Louisville, University of Louisville, Louisville, KY, 40202.

2. Poster presentation, D. Gomes, J. Zhao, M.S. Kumar, M. Subheeswar, A. Amraotkar, T.E. O'Toole. "Does Carnosine protect against the adverse effects of PM2.5 exposure? The Nucleophillic Defense against PM toxicity (NEAT) trial", Research Louisville, University of Louisville, Louisville, KY, 40202.

2. Poster presentation, D. Gomes, B.J. Ulrich, M. H. Kaplan. "Heterogeneity in TH9 cultures", Joseph Moore Museum Science Communication poster presentations, Earlham College, Richmond, IN, 47374.

3. Poster presentation, L. Pegram, D. Gomes, A. Mishra, C. Buckman. "Contrasting the Hoffmeister effects of GuHCl and KCl", Joseph Moore Museum Science Communication poster presentations, Earlham College, Richmond, IN, 47374.

4. Poster presentation, D. Gomes, E. PenaCalderin, J. Zhang, Z. Wohl, M. Nystoriak. "Investigation and characterization of mRNA transcript levels and protein-protein interactions in mouse coronary artery cells using RNA-ISH and proximity ligation assay", Joseph Moore Museum Science Communication poster presentations, Earlham College, Richmond, IN, 47374.

### Publications

1. Publication, Zhao, J., Gomes, D., Jin, L., Mathis, S. P., Li, X., Rouchka, E. C., Bodduluri, H., Conklin, D. J., & O'Toole, T. E. (2022). Polystyrene bead ingestion promotes adiposity and cardiometabolic disease in mice. Ecotoxicology and environmental safety, 232, 113239.